Research Square

Preprints are preliminary reports that have not undergone peer review.
They should not be considered conclusive, used to inform clinical practice,
or referenced by the media as validated information.

The Slow Side of AMPA Dynamics: A Parsimonious Framework for TARP-Dependent Receptor Kinetics

Brian Skelly
University College Dublin
Áine Byrne
aine.byrne@ucd.ie

University College Dublin

Research Article

Keywords: AMPA, TARPs, slow AMPA, kinetic modelling, biophysics

Posted Date: June 26th, 2026

DOI: https://doi.org/10.21203/rs.3.rs-9972009/v1

License: This work is licensed under a Creative Commons Attribution 4.0 International License.
Read Full License

Additional Declarations: No competing interests reported.

The Slow Side of AMPA Dynamics: A Parsimonious Framework for TARP-Dependent Receptor Kinetics

Brian Skelly[1] and Áine Byrne[1*]

[1]School of Mathematics and Statistics, University College Dublin, Belfield, Dublin 4, Ireland.

*Corresponding author(s). E-mail(s): aine.byrne@ucd.ie;
Contributing authors: brian.skelly@ucdconnect.ie;

Abstract

AMPA receptors (AMPARs) are the primary mediators of fast excitatory neurotransmission throughout the brain. Their biophysical dynamics are modulated by Transmembrane AMPAR Regulatory Proteins (TARPs), which are found in varying proportions across the brain. Despite the functional diversity, standard computational models of neural activity often rely heavily on simplified conductance equations that fail to capture variable synaptic dynamics. To address this limitation, we develop and validate a reduced model of AMPARs capable of simulating TARPless and TARPed states through simple parameter changes. Integrating this into a single neuron model, our simulations reveal that unlike neurons with TARPless receptors, neurons with TARPed receptors successfully fire during relatively low frequency stimulations. These findings demonstrate how variable TARP expression shapes neuronal output. Furthermore, as abnormal TARP activity is linked to specific forms of epilepsy, this computationally efficient model provides a valuable tool for investigating the mechanisms underlying pathological network excitability.

Keywords: AMPA, TARPs, slow AMPA, kinetic modelling, biophysics

1 Introduction

Synaptic transmission in the brain is mediated primarily by chemical synapses [1]. The efficiency of information processing within these neural circuits depends both on

the strength of synaptic connections and the precise temporal dynamics. Disruptions in synaptic function can lead to pathological brain activity, such as seizures, and many neurodevelopmental disorders and neurodegenerative diseases are associated with dysregulation of synapses [2].

The predominant receptor type for excitatory synapses is the α-amino-3-hydroxy-5-methyl-4-isoxazolepropionic acid (AMPA) receptor [3], which is a glutamate gated ion channel. Traditionally, AMPA receptors are viewed as the primary mediators of fast excitatory neurotransmission [4]. Structurally, they are tetramers composed of four subunits, where the binding of glutamate to these subunits triggers the opening of ion channels. As glutamate binds to more subunits, the receptor allows a larger influx of ions, leading to higher levels of conductance [5, 6].

More recently, AMPA receptors have been shown to exhibit slow dynamics in the presence of Transmembrane AMPA receptor regulatory proteins (TARPs) [7–13]. These auxiliary proteins bind to the receptors and alter their gating kinetics. Specifically, TARPs decrease the ion channel closing rate by roughly 100-fold, significantly increasing the amount of time spent in the open state. They also lower the desensitisation rate and increase the binding rate for additional subunits [10]. This results in *superactivation*, a prolonged increase in conductance [9], where the typical decay time increases by up to two orders of magnitude from ~ 5 ms to $100 - 500$ ms [14]. Such slow dynamics are particularly common in the CA3 region of the hippocampus, where roughly one-third of receptors are TARPed [8]. The magnitude of this kinetic modulation is subtype-dependent, with TARP $\gamma - 4$ and $\gamma - 8$ isoforms exerting the most pronounced superactivating effects.

To capture these conformal changes, synaptic receptors are commonly modelled using kinetic, state-based schemes where the receptor transitions between discrete states according to Markov processes [5, 10, 13, 14]. While these models provide a rigorous biophysical framework, there is no universal consensus on the necessary number of states or permitted transitions. Although high-dimensional models, encompassing numerous open, closed, and desensitized states, offer granular detail, such complexity often leads to over-parameterisation. Consequently, parsimonious kinetic schemes are generally preferred; utilizing the minimal number of states necessary to robustly replicate empirical data ensures both analytical tractability and computational efficiency [5, 10].

An alternative approach are phenomenological models that reproduce observed synaptic dynamics without explicitly describing the underlying kinetic states. The simplest of these include first-order exponential decays and alpha functions, which describe synaptic conductance as a delayed rise followed by an exponential decay. More biologically descriptive formulations, such as the Tsodyks-Markram (TM) framework [15], introduce finite resource variables to successfully capture activity-dependent short-term plasticity, including synaptic depression and facilitation. Although computationally simple, they assume a constant decay rate, and as such,

cannot capture TARP-mediated superactivation and the associated prolongation of deactivation kinetics.

In this paper, we present a biophysical modelling framework for synaptic coupling grounded in receptor state occupancies. We construct and validate a deterministic ordinary differential equation (ODE) model describing receptor state occupancies based on Milstein *et al.*'s 8-state Markovian kinetic scheme [10]. Given the computational intractability of high-dimensional kinetic models in large-scale network simulations, we then derive a computationally efficient, phenomenological reduced model inspired by the TM formalism [15], and fit its parameters to match the behaviour of the full kinetic model. We demonstrate that the reduced model captures the defining features of slow AMPA receptors, including superactivation, substantially longer decay times, and recovery from desensitisation.

2 Methods

In this section, we detail the transition from a high-dimensional, biophysical representation of the AMPA receptor to a computationally efficient reduced model. We use the 8-state Markovian kinetic scheme originally proposed by Milstein *et al.* [10] as a benchmark for our reduced model, comparing the time courses for the synaptic conductance. Finally, we detail how we incorporate this optimised reduced model into the Hodgkin-Huxley neuronal architecture to assess the impact of TARPs on postsynaptic voltage dynamics.

Kinetic model

To establish a biophysical baseline, we employ the 8-state model of Milstein *et al.* [10], with two sets of open, closed and desensitised states (see Fig. 1). The two levels of states correspond to the binding of either three or four glutamate molecules to the tetrameric subunits. We note that further simplifications aggregating these into single open, closed, and desensitized states, such as the model proposed by Cho *et al.* [12], failed to capture the required slow dynamics.

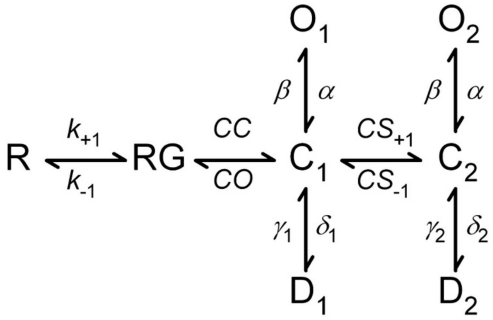

Fig. 1 Kinetic scheme. Schematic illustrating the 8 states of the receptor, with arrows indicating the transition rates between different states.

While traditional continuous-time Markov chains provide a highly detailed stochastic framework, this level of detail is not required here. Instead, we constructed a deterministic approximation of the Milstein scheme, hereafter referred to as the Kinetic Receptor (KR) model. The KR model describes the fractional occupancy of receptors in each state:

$$\frac{dR}{dt} = k_{-1}R_G - G(t)k_{+1}R, \tag{1}$$

$$\frac{dR_G}{dt} = G(t)k_{+1}R - k_{-1}R_G + C_O C_1 - dC_C R_G, \tag{2}$$

$$\frac{dC_1}{dt} = C_C R_G - C_O C_1 + \alpha O_1 - \beta dC_1 + \gamma_1 D_1 - \delta_1 C_1 + CS_{-1}C_2 - CS_{+1}C_1, \tag{3}$$

$$\frac{dO_1}{dt} = \beta C_1 - \alpha O_1, \tag{4}$$

$$\frac{dD_1}{dt} = \delta_1 C_1 - \gamma_1 D_1, \tag{5}$$

$$\frac{dC_2}{dt} = CS_{+1}C_1 - CS_{-1}C_2 + \alpha O_2 - \beta C_2 + \gamma_2 D_2 - \delta_2 C_2, \tag{6}$$

$$\frac{dO_2}{dt} = \beta C_2 - \alpha O_2, \tag{7}$$

$$\frac{dD_2}{dt} = \delta_2 C_2 - \gamma_2 D_2. \tag{8}$$

Here, variables represent the proportion of receptors in the unbound R, glutamate-bound RG, closed $C_{1,2}$, open $O_{1,2}$, and desensitised $D_{1,2}$ states. Transition rates (k_{-1}, CC, CO, CS_{+1}, CS_{-1}, α, β, γ_1, δ_1, γ_2, δ_2) are given in s^{-1} with the exception of k_{+1} which has units Ms^{-1}. The external drive, $G(t)$, represents the transient synaptic glutamate concentration. The synaptic conductance is then given as,

$$s_{syn}^{KR}(t) = O_1 + 2O_2. \tag{9}$$

Reduced model

Inspired by the Tsodyks and Markram (TM) [15] model of short-term plasticity, we develop a reduced model of synaptic transmission which supports the key features of superactivation. Like the TM model, we include a resource factor X and utilisation factor U, but we extend the synaptic current dynamics to include a fast (s_{fast}) and a

slow component (s_{slow}),

$$\begin{aligned}
\frac{dX}{dt} &= \frac{1-X}{\tau_X} - \alpha U X G(t), \\
\frac{dU}{dt} &= \frac{U_0 - U}{\tau_U} + U_0(1-U)G(t), \\
\frac{ds_{fast}}{dt} &= \frac{-s_{fast}}{\tau_{fast}} + A_1 U X G(t), \\
\frac{ds_{slow}}{dt} &= \frac{-s_{slow}}{\tau_{slow}} + A_2 U X G(t).
\end{aligned} \tag{10}$$

Here, τ_X and τ_U are the timescales of depression and facilitation, respectively, and τ_{fast} and τ_{slow} are the fast and slow, respectively, synaptic timescales. The coefficients α, A_1, and A_2 scale the response amplitude upon glutamate stimulation, while U_0 defines the baseline synaptic efficacy. The external input, $G(t)$, again corresponds to the transient glutamate concentration, which can be thought of as an applied glutamate pulse or glutamate release as a result of an incoming action potential. The synaptic conductance is then computed as the superposition of the fast and slow components

$$s_{syn}^{Reduced}(t) = s_{fast} + s_{slow}. \tag{11}$$

By explicitly separating the conductance into fast and slow components (s_{fast} and s_{slow}), this 4-variable model gains the necessary degrees of freedom to replicate the delayed deactivation and prolonged pedestal currents characteristic of TARP-bound AMPA receptors.

Stimulation Protocols

To ensure the physiological relevance, we evaluated the ability of both models to replicate fundamental kinetic features observed in experimental studies. Specifically, we employ three different stimulation protocols: single pulse stimulation, train stimulation, two pulse protocol.

1. **Single pulse stimulation:** Experimental studies show that the synaptic conductance rises rapidly, before decaying back to zero, in response to the application of glutamate. The time to decay back to zero is dramatically increased from roughly 5 ms for TARPless receptors up to 500 ms for TARPed receptors (Fig. 2A). To model the single pulse stimulation, we define the external input $G(t)$ as a single pulse of height 0.001 (corresponding to 1 mM) and width 1 ms starting at $t = 0$, i.e. $G(t) = 0.001\Theta(x)\Theta(1-x)$, where $\Theta(x)$ is the Heaviside function.
2. **Train stimulation:** In response to a series of pulses, commonly referred to as a *train*, the synaptic conductance for TARPless receptors exhibits depression, where the height of the peaks in conductance are smaller for subsequent glutamate pulses (Fig. 2B). The extent of this decay depends on the stimulation frequency. For TARPed receptors, we see superactivation, where the conductance does not return to zero between pulses and, as such, the height of the peaks do not decay, and for

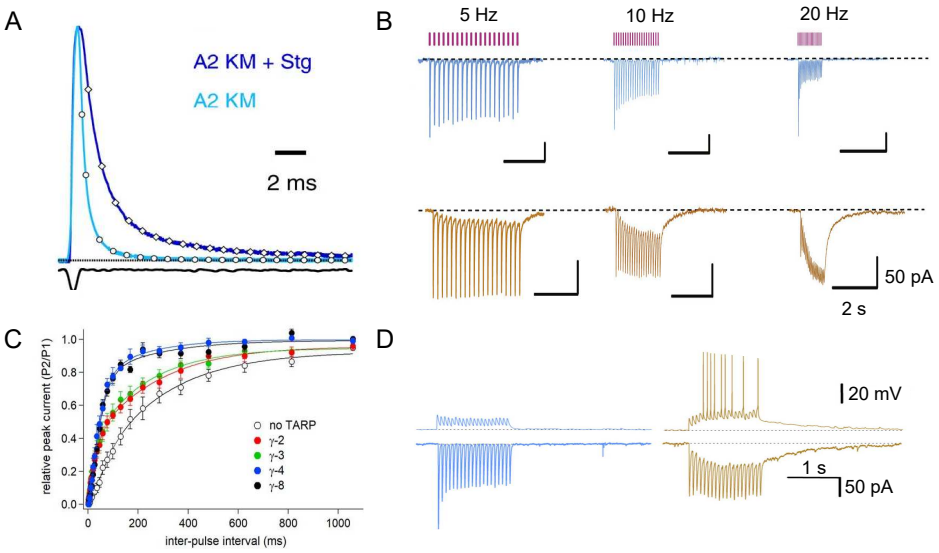

Fig. 2 Key AMPA receptor dynamics observed experimentally. A. Response to a single pulse, illustrating the increased rate of decay for TARPed receptors (dark blue) compared to TARPless receptors (light blue). Modified from [14]. **B.** Train stimulation results, showing depression for TARPless receptors (blue) and superactivation for TARPed receptors (orange) at both 5 Hz and 20 Hz. Modified from [8]. **C.** Two pulse protocol results, showing the recovery of the receptor from desensitisation is faster for TARPed receptors (coloured dots) compared to TARPless receptors (white). Modified from [7]. **D.** Neuronal response, showing the conductance (bottom traces) and corresponding voltage response (top traces) to a high frequency input for TARPless (blue) and TARPed (orange) receptors. Modified from [8].

high frequencies they may even increase. To model this scenario, we let $G(t)$ be a series of 20 pulses of height 0.001 and width 1 ms, where the time between pulses is determined by the stimulation frequency f as $1000/f$. Mathematically, this can be written as $G(t) = 0.001 \sum_{n=0}^{19} \Theta\left(x - \frac{1000}{f} n\right) \Theta\left(\frac{1000}{f} n + 1 - x\right)$.

3. **Two pulse protocol:** The two pulse protocol involves applying a 10 mM glutamate pulse for 50 ms to fully desensitise the synapse (all receptors in the desensitised state), and then applying a second pulse at various inter-stimulation intervals to assess the recovery of the receptors from desensitisation. When no TARPs are present the receptors require at least 1 second to fully recover (ratio of peaks approaches 1) (white circles in Fig. 2C). While for TARPed receptors, the receptors recover more quickly and, for γ_4 and γ_8 in particular, the ratio of the peaks approaches 1 after 200-300 ms (blue and black circles in Fig. 2C). For the protocol, we employ two 0.01 M $\times$ 50 ms pulses with an inter-stimulation interval of Δ, i.e. $G(t) = 0.01\left(\Theta(x)\,\Theta(50 - x) + \Theta(x - 50 - \Delta)\,\Theta(100 + \Delta - x)\right)$.

Parameter fitting

The parameter fitting process was conducted in two stages: first, adjusting the biophysical constants of the Kinetic Receptor (KR) model to reflect TARP-mediated

changes, and second, utilising numerical optimisation to align the reduced model with the KR model's behaviour.

Kinetic Model Calibration

We use the parameters of Milstein *et al.* [10] as a baseline for the KR model. However, Milstein *et al.* fit the parameters to match the response to single pulse experiments only. To achieve the recovery from desensitisation time frame seen in other experiments [14, 16] we needed to increase γ_1 and γ_2 by a factor of 3 for both the TARPless and TARPed cases. Increasing γ_1 and γ_2, which control the rate at which the receptor recovers from desensitisation, was particularly important for the 2 pulse protocol experiments. To achieve superactivation, we also had to increase the activation rate β for TARPed receptors. (Note that we are not fitting to a specific TARP, but rather aiming to reproduce the general behaviour of TARPed receptors.) In increasing β we effectively increase the probability of being in the open state, which creates a more pronounced "pedestal" in the current for TARPed receptors. All other parameters are the same as in [10]. All parameter values are given in Table 1. With these parameter values, we achieve dynamics similar to the experimental findings (Fig. 2) for each of the stimulation protocols (see Section 3).

Reduced Model Optimization

To fit the parameters of the reduced model, we performed a global optimisation, utilising the `differential_evolution` function from `scipy.optimize`, to minimise the difference between the time courses of the synaptic conductance for the reduced model and the kinetic model. As this is a global minimisation package, the final results are independent of initial parameter values. To ensure stability and account for potential non-unique minima, the optimiser was run 30 times to confirm convergence on a consistent global minimum.

The optimisation was split into two parts. First, we study the response to a single pulse stimulation (see Stimulation Protocols above). For a single stimulation, the resource X and utilisation U factors do not impact the dynamics of s_{fast} and s_{slow}, apart from their initial values. Hence, we only fit the parameters τ_{fast}, τ_{slow}, A_1, and A_2 at this stage. To capture the long deactivation tails of TARPed receptors, a log-transformed least-squares approach was employed. Additionally, a constant penalty was applied if the peak amplitude fell outside 95%–110% of the KR model's amplitude to prevent the optimiser from over-prioritising decay at the expense of the initial response. The objective function is as follows

$$\min\left(\sum_i \left[\ln(s_{syn}^{KR}(t_i)) - \ln(s_{syn}^{Reduced}(t_i))\right]^2 + \text{penalty}\right)$$

$$\text{penalty} = \begin{cases} 0 & \text{for} \quad 0.95 < \dfrac{\max(s_{syn}^{KR}(t))}{\max(s_{syn}^{Reduced}(t))} < 1.10, \\ 50 & \text{otherwise.} \end{cases}$$

With the synaptic conductance parameters fixed, we fit the resource and facilitation parameters (τ_X, τ_U, and U_0) using the response to train stimulations (see Stimulation Protocols above). We initially fit the model parameters for different stimulation frequencies separately, and found that the optimal parameter values depended on the stimulation frequency. Hence, we decided to run one long simulation with 300 ms blocks of different stimulation frequencies, namely, 5 Hz, 10 Hz, 20 Hz, 50 Hz, 100 Hz, 200 Hz, 300 Hz, 400 Hz, and 500 Hz. This gave us a single time course to efficiently optimise the parameter values across all stimulation frequencies. The objective function used here is

$$\min\left(\sum_i \left[s_{syn}^{KR}(t_i) - s_{syn}^{Reduced}(t_i)\right]^2\right).$$

During this process, we fixed $\alpha = 1$ to avoid non-unique solutions that occurred when optimising α and U_0 simultaneously. The resulting parameters (given in Table 1) show that TARPed receptors exhibit slower fast-component decays (τ_{fast} larger), higher contributions from slow-decay components (A_2 larger), and faster resource recovery times (τ_X smaller), reflecting the reduced desensitisation seen for TARPed receptors in the kinetic model.

		Median	[min, max]
τ_{fast}	TARPless	0.92878	[0.92878, 0.92879]
	TARPed	9.0283	[9.0271, 9.0309]
τ_{slow}	TARPless	402.80	[399.67, 405.64]
	TARPed	64.515	[64.514, 64.517]
A_1	TARPless	1.5394	[1.5394, 1.5394]
	TARPed	1.2318	[1.2317, 1.2318]
A_2	TARPless	0.0015194	[0.0015183, 0.0015202]
	TARPed	0.23848	[0.23846, 0.23851]
τ_X	TARPless	426.06	[410.36, 434.12]
	TARPed	58.250	[57.958, 59.607]
τ_U	TARPless	0.66711	[0.50579, 0.70149]
	TARPed	0.56018	[0.50040, 0.58685]
U_0	TARPless	0.62728	[0.60854, 0.66677]
	TARPed	0.93773	[0.92788, 0.94596]

Table 1 Optimised parameters for both TARPless and TARPed receptors. The third column shows the median value found to five significant figures and the fourth column shows the interval from the minimum to maximum values found by the optimiser to five significant figures.

Neuron model

To assess how TARPed AMPA receptors influence neuronal output, we integrated the reduced model into a single-cell framework using a Hodgkin-Huxley (HH) model neuron [17]. This transition allows us to quantify how the shift from fast to slow

synaptic kinetics modulates membrane potential and firing thresholds. In particular, Pampaloni *et al.* found that the increased conductance from bound TARPs increases the excitability of the neuron [8], leading to spikes which are not seen in the TARPless case (Fig. 2D).

We modify the classic Hodgkin-Huxley voltage equations to include an additional term for the synaptic current:

$$C_m \frac{dv}{dt} = -\Big(I_{Na} + I_K + I_L\Big) + I_{ext} + k s_{syn}(v_{syn} - v)$$

where v is the membrane potential, I_{Na}, I_K, and I_L are the dynamic ionic currents, I_{ext} is the external background drive, k is the synaptic coupling strength, v_{syn} is the synaptic reversal potential, s_{syn} is the synaptic conductance (given by (11) for the reduced model). Full model equations and parameter can be found in Appendix A.

To fit the synaptic coupling strength k, we note that Pampaloni *et al.* found a roughly 12 mV excitatory postsynaptic potential (EPSP) after the first stimulation pulse [8]. We set I_{ext} such that $v \approx -67$ mV in the absence of synaptic input, as Pampaloni *et al.* voltage clamped experiments were set at this value, and then measured the voltage increase following a 1 mM glutamate pulse applied for 1 ms and calibrated k such that the voltage increase was 12 mV. Based on the results of Pampaloni *et al.*, we conclude that the initial 12 mV response is the same for both TARPless or TARPed receptors, and set $k_{TARPless} = 0.3$ and $k_{TARPed} = 0.03$ to match this initial response.

In order to replicate the irregular spiking observed in real data, we introduced independent Poisson noise. At each times-step, the variables v, s_{fast} and s_{slow} are driven by Poisson inputs with specific amplitudes 0.1, 0.02, and 0.0001, respectively, and rates 3 ms^{-1}, 0.05 ms^{-1}, and 0.01 ms^{-1}. This stochasticity allows the neuron to cross the spiking threshold more realistically. Through this model, we examine how the enhanced conductance characteristic of TARPed receptors directly alters the membrane's response to synaptic input.

3 Results

Kinetic Model

To ensure that our deterministic model matched the Monte Carlo system for a high number of receptors, we first compare the Monte Carlo dynamics to the deterministic ODE model for different numbers of receptors. We found that the ODE model accurately reproduced the results of the Markov simulations, with the accuracy improving as the number of receptors included in the Markov simulations is increased (Fig. 3). We show that the solutions of the ODE model (dashed black) more closely match the Markov simulations results for 50000 receptors (orange), compared to 1000 receptors (purple) which show significantly more variability across runs (five sample solutions are shown for each).

Although the KR model is biophysically accurate, it would prove computationally expensive for large networks of interconnected neurons. Simulating network of N

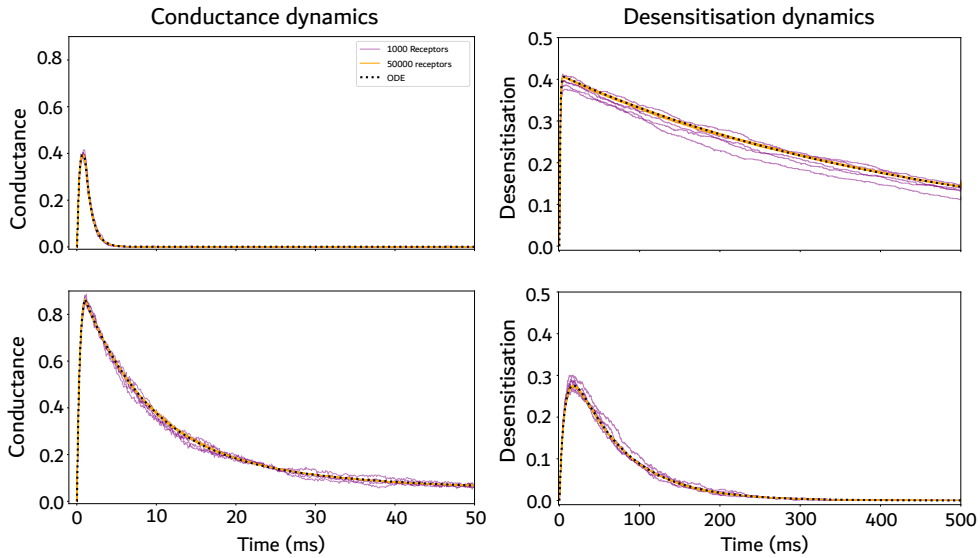

Fig. 3 Validation of the deterministic ODE model. Comparison of the Monte Carlo style kinetic scheme to our ODE model, showing five different Monte Carlo simulations of 1000 receptors (purple) and of 50000 receptors (orange), as well as for the ODE model (dashed black). It is clear that ODE model accurately tracks the kinetics for a sufficiently large number of receptors. (Left) The synaptic conductance $s_{syn}^{KR}(t)$ (9) for TARPless receptors (top) and TARPed receptors (bottom). (Right) Proportion of channels in the desensitised states D_1+D_2 for TARPless receptors(top) and TARPed receptors (bottom).

coupled neurons would require tracking N^2 synaptic connections, i.e. N^2 sets of eight ODEs. To reduce this cost, we propose a reduced model with half the number of equations per synapse while preserving the key features of superactivation.

Single Pulse stimulation

We found that both models could accurately reproduce the conductance dynamics for a single pulse of glutamate whether TARPless or TARPed (Fig. 4). As seen experimentally, the decay time for the synaptic conductance is roughly ~ 5 ms for TARPless receptors and ~ 200 ms for TARPed receptors.

When fitting the reduced model parameters, we prioritised matching the decay kinetics rather than the initial amplitude of the response to a single stimuli. Therefore, we see that the reduced model (dashed orange in Fig. 4) has a higher amplitude than that of the KR model (purple). However, the decay profiles are very closely matched, which is more important.

Train stimulation

The second experiment looks at the conductance in response to a train of stimulations (Fig. 5). We found that both the KR model (purple) and our reduced model (dashed orange) could accurately produce the differences between TARPless and TARPed

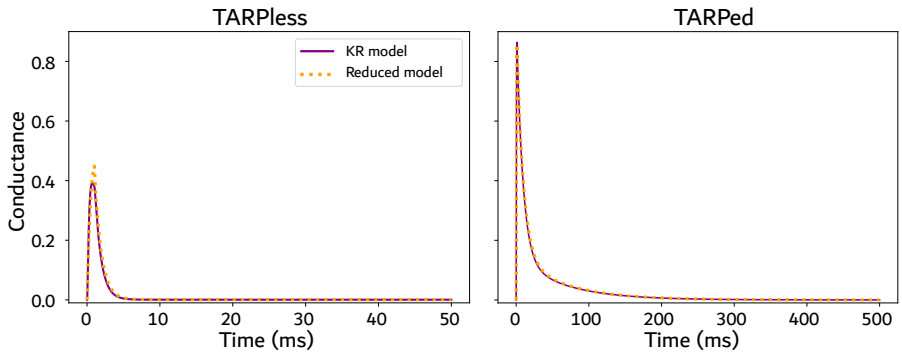

Fig. 4 Single Pulse stimulation. The reduced model (dashed orange) display similar decay kinetics to the KR model (purple) in response to a 1 ms 1 mM pulse of glutamate. As expected, it takes much longer for the TARPed (right) conductance to decay back to zero than the TARPless (left). Note the different timescales of the TARPless and TARPed plots.

AMPA receptors dynamics across a range of different stimulation frequencies. In particular, we observe a significant amount of superactivation for fast stimulation of the TARPed receptors (Fig. 5 bottom right), which is not present in the TARPless case (Fig. 5 bottom left). In each case, we see that the peak conductance values are slightly different for the reduced model compared to the KR model. However, the total conductance (area under the curve) are similar. For example, for the 20 Hz TARPed case, the total conductance is 319.691 for the reduced model and 309.512 for the KR model, which gives a relative error of 3.29%, indicating very similar mean synaptic response.

Two pulse protocol

Next we employed the two pulse protocol to evaluate the models' recovery from desensitisation and validate the parameter optimisation. All parameter values are now fixed and no further optimisation was carried out to match the dynamics of the two models. As outlined in Section 2, this protocol involves a conditioning pulse (10 mM glutamate for 50 ms) designed to drive the majority of receptors into desensitised states, followed by a second test pulse at varying inter-pulse intervals (Δ).

In the TARPless configuration (solid lines), both the Kinetic Receptor (KR) model (purple) and the reduced model (orange) exhibit a characteristic saturating recovery curve (Fig. 6). Complete recovery, where the peak conductance of the second pulse matched the first, requires a recovery interval exceeding 1 second, as seen experimentally (Fig. 2D). In contrast, the inclusion of TARPs significantly accelerated this process, with full recovery occurring within 200–300 ms. Furthermore, TARPed receptors only reached approximately 60% desensitisation even after the prolonged conditioning pulse, whereas TARPless receptors were nearly fully desensitised. This property allows TARPed synapses to maintain a consistent baseline conductance during high-frequency activity, a feature notably absent in the rapidly desensitising TARPless models. We note that the peak ratio does not go to zero (as seen in the experimental results, Fig. 2D), as we chose to compute the peak ratio at all inter-pulse

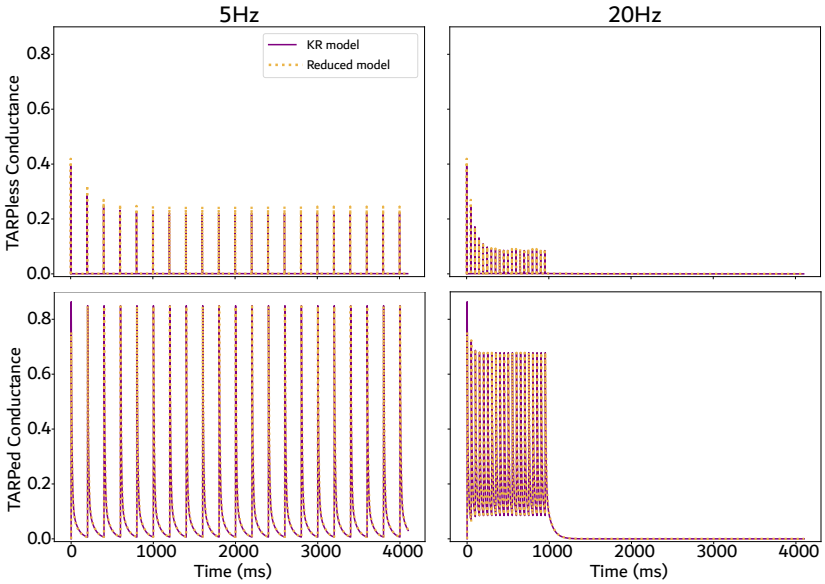

Fig. 5 Train stimulation. For both the 5 Hz (left) and 20 Hz (right) train stimulation, the reduced model (dashed orange) accurately reproduces the key dynamics as the KR model (purple). We observe synaptic depression for the TARPless receptors (top), with the peak response decreasing for each subsequent pulse. The conductance is significantly greater for the TARPed receptors (bottom), exhibiting characteristics of superactivation.

intervals, rather than employing the work around used by Devi *et al.* [14] for measuring the height of the second pulse when the conductance is still high from the first pulse (inter-pulse interval of less that 100 ms).

Modulation of Neuronal Excitability by TARPs

Finally, we investigate how TARPs affect the membrane potential and overall excitability of neurons, by integrating the reduced model for synaptic conductance into a Hodgkin-Huxley neuron model (outlined in Section 2). For both the TARPless and TARPed dynamics, the repeated stimulation on the receptors results in rapid increases in the membrane potential of roughly 12 mV. In the absence of TARPs, the membrane potential quickly decays towards the resting potential after each stimulation, whereas TARPs slow down this decay. For low stimulation frequencies, the qualitative behaviour of the membrane potential in each case is similar. However, as the stimulation frequency is increased, the slow decay of the membrane potential in the TARPed case results in a gradual increase of the peak membrane potential at each stimulation, bringing it closer and closer to threshold and ultimately triggering an action potential every 5-6 stimulations. These results demonstrate that TARPs directly modulate neuronal output by enhancing the excitability and firing rate of the post-synaptic cell, consistent with experimental findings [10, 12, 18].

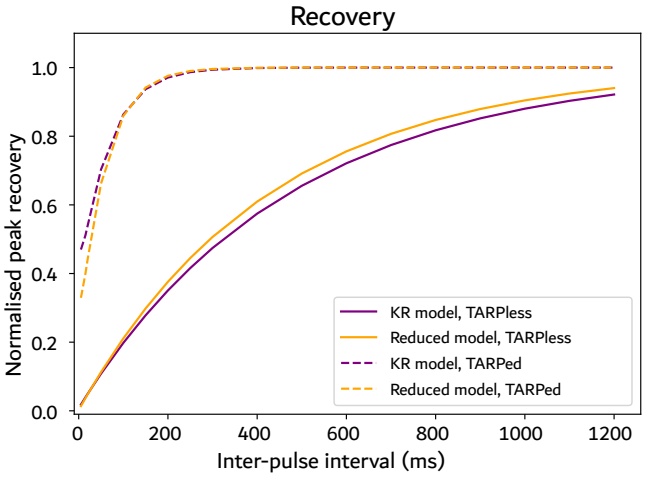

Fig. 6 Two pulse protocol. The recovery of the reduced model follows a qualitatively similar trajectory to the more high-dimensional KR model in both the TARPless ad TARPed cases. When TARPed, less receptors become desensitised, and they recover quicker.

4 Discussion

Recent experimental evidence has demonstrated that Transmembrane AMPA Receptor Regulatory Proteins (TARPs) significantly alter the opening and closing kinetics of AMPA receptors. By slowing deactivation and reducing desensitisation, TARPs modulate both the speed of synaptic transmission and neuronal excitability. Given that dysregulated excitatory dynamics are fundamentally linked to the pathogenesis of conditions such as epilepsy, the development of accurate, computationally efficient models of TARP-dependent kinetics is critical for conducting disease-relevant network simulations [19, 20].

In this study, we successfully adapted a high-dimensional Markovian receptor model into a deterministic system of ordinary differential equations (ODEs). This Kinetic Receptor (KR) model serves as a biophysical benchmark for simulating the distinct behaviours of traditional "fast" AMPA receptors, as well as the "slow" dynamics characteristic of TARPed receptors, including phenomena such as superactivation and accelerated recovery from desensitisation. While functionally accurate, the KR model remains computationally expensive for network-level studies, requiring eight ODEs per synapse. To address this, we developed a 4-variable reduced model that can reproduce all of the key feature of TARPless and TARPed receptors. By reducing the number of state variables by 50%, our model significantly lowers the computational cost of simulating networks with $\mathcal{O}(N^2)$ synaptic connections without sacrificing the essential deactivation profiles or the ability to maintain a baseline pedestal current.

Integrating the reduced model for receptor dynamics into a Hodgkin-Huxley neuron model confirmed that the presence of TARPs increases the firing rate of individual neurons, a finding that aligns with established experimental data [10, 12, 18] This framework provides a scalable foundation for future research into how heterogeneous

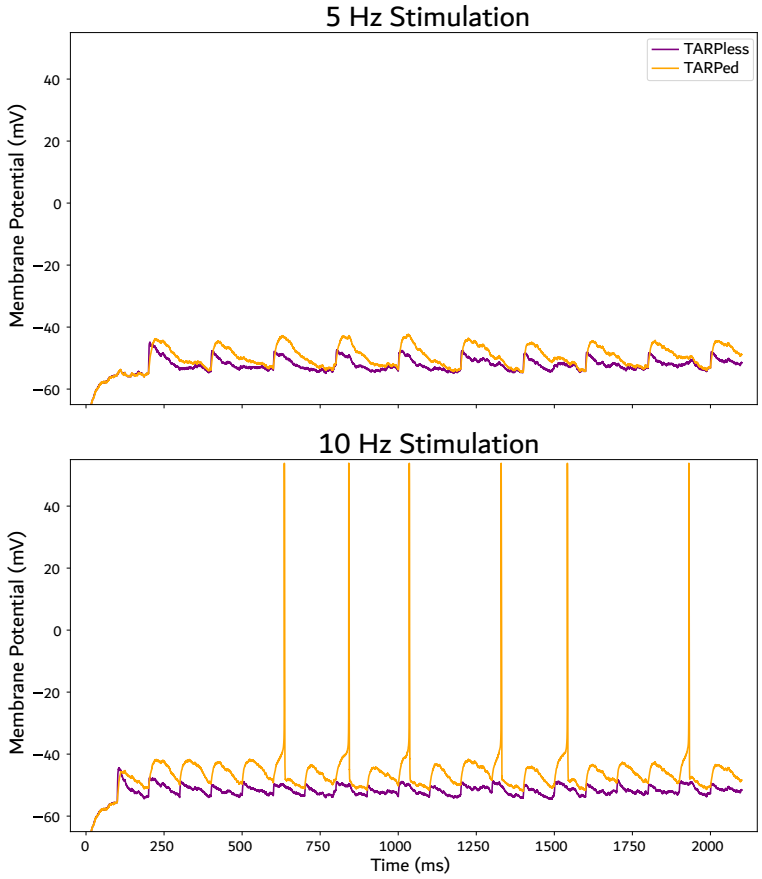

Fig. 7 TARPs enhance neuronal excitability. Membrane potential in response to a 5 Hz (top) and a 10 Hz (bottom) stimulation, for TARPless receptors (purple) and TARPed receptors (orange). The slow decay of the membrane potential post-stimulation results in a temporal summation of the responses, and for high stimulation frequencies, the membrane potential reaches the firing threshold and an action potential is triggered.

TARP concentrations, such as the distribution of TARP γ-2 in the cerebellum versus γ-4 or γ-8 in the cerebral cortex [14], influence global network properties like synchronous firing and seizure thresholds. This is of particular clinical importance, as TARP γ-8 inhibitors are currently being investigated as potential anti-epileptic therapies to modulate hyperexcitability [19, 21]. Our model offers a valuable tool for simulating the effects of such pharmacological interventions.

Beyond its current implementation, the model offers opportunities for further parsimonious reduction. In cases where only TARPless receptors are considered, we found that the slow conductance variable (s_{slow}) could be eliminated due to its negligible scaling factor. Additionally, since the facilitation timescale (τ_U) is orders of magnitude

faster than the depression timescale (τ_X), the utilisation variable (U) could potentially be replaced with a constant scaling factor without significantly compromising accuracy, particularly during sustained high-frequency stimulation.

While the current reduced model captures generalised TARPed behaviour, it is not yet specific to individual TARP subtypes. However, the underlying KR model is sufficiently flexible to be re-parameterised for specific configurations, such as GluA1/TARP γ-2 or γ-8 combinations. We also observed that the model maintains a residual conductance under extreme, sustained glutamate stimulation rather than desensitising completely. While this diverges slightly from some in vitro observations, such sustained concentrations (e.g., 10 mM for 50 ms) are unlikely to occur in vivo, where glutamate peaks at approximately 1 mM and is cleared rapidly following an action potential. Consequently, our model remains a robust and physiologically relevant representation of synaptic dynamics under naturalistic conditions.

In summary, we have developed a computationally efficient model of synaptic transmission that accurately captures the complex, TARP-dependent gating kinetics of AMPA receptors. By bridging the gap between high-dimensional biophysical Markov models and simplified neuronal simulations, this work provides a practical tool for exploring the functional consequences of synaptic "superactivation". Future work will aim to embed our synaptic model into large-scale neural networks and explore how the introduction of slow AMPA currents (TARPed receptors) affects network dynamics, focusing on the transition from normal physiological activity to pathological hyperexcitability and seizure-like states. As research continues to uncover the role of specific TARP isoforms in neurodegenerative disorders, this modelling framework offers a scalable foundation for simulating targeted pharmacological interventions and understanding the emergent properties of complex, excitable neural networks.

Acknowledgements. We thank Marcel Goldschen for his help in understanding the Milstein's kinetic scheme, and the role of glutamate on this model.

Appendix A Hodgkin-Huxley model

Below are the equations for the Hodgkin-Huxley neuron model that were used.

$$
\begin{aligned}
C_m \frac{dv}{dt} &= -g_{Na} m^3 h (v - E_{Na}) - g_K n^4 (v - E_K) - g_L (v - E_L) + I_{ext} + k s_{syn} (v_{syn} - v) \\
\frac{dm}{dt} &= \alpha_m (1 - m) - \beta_m m, \\
\frac{dn}{dt} &= \alpha_n (1 - n) - \beta_n n, \\
\frac{dh}{dt} &= \alpha_h (1 - h) - \beta_h h,
\end{aligned}
$$

where v is the membrane potential, g_i are the maximal conductances, E_i are the reversal potentials, and m, n, and h are the gating variables describing the opening and closing probabilities of sodium and potassium channels (see below). The activation of the potassium channel is denoted by n, while m and h represent the activation

and inactivation of the sodium (Na^+) channel respectively. The background current is given as I_{ext}, and the synaptic current has synaptic strength k, conductance s_{syn}, and reversal potential v_{syn}. The opening and closing functions α_i and β_i are given as

$$\alpha_n = \frac{-0.032(v - v_t - 15)}{\exp(-(v - v_t - 15)/5) - 1},$$
$$\beta_n = 0.5 \exp(\frac{-(v - v_t - 10)}{40}),$$
$$\alpha_m = -0.32 \frac{v - v_t - 13}{\exp(-\frac{v - v_t - 13}{4} - 1},$$
$$\beta_m = 0.28 \frac{v - v_t - 40}{\exp(\frac{v - v_t - 40}{5}) - 1},$$
$$\alpha_h = 0.128 \exp(-\frac{v - v_t - 17}{18}),$$
$$\beta_h = \frac{4}{1 + \exp(-\frac{v - v_t - 40}{5})}.$$

The value for each parameter is given in Table A1.

parameters	values
C_m	1
g_{na}	60
v_{syn}	0
g_k	3
E_{na}	55
g_l	0.025
E_k	-80
v_t	-45
E_l	-70

Table A1 Parameter values used in single neuron simulations

References

[1] Hestrin, S.: The strength of electrical synapses. Science **334**(6054), 315–316 (2011) https://doi.org/10.1126/science.1213894 https://www.science.org/doi/pdf/10.1126/science.1213894

[2] Bowie, D.: Ionotropic glutamate receptors & cns disorders. CNS & Neurological Disorders - Drug Targets **7**(2), 129–43 (2008) https://doi.org/10.2174/187152708784083821 . https://www.ncbi.nlm.nih.gov/pmc/articles/2662616

[3] Platt, S.R.: The role of glutamate in central nervous system health and disease – a review. The Veterinary Journal **173**(2), 278–286 (2007) https://doi.org/10.1016/j.tvjl.2005.11.007

[4] Stafford, B.K., Manookin, M.B., Singer, J.H., Demb, J.B.: Nmda and ampa receptors contribute similarly to temporal processing in mammalian retinal ganglion cells. The Journal of Physiology **592**(22), 4877–4889 (2014) https://doi.org/10.1113/jphysiol.2014.276543 https://physoc.onlinelibrary.wiley.com/doi/pdf/10.1113/jphysiol.2014.276543

[5] Zhang, W., Robert, A., Vogensen, S.B., Howe, J.R.: The relationship between agonist potency and ampa receptor kinetics. Biophysical Journal **91**(4), 1336–1346 (2006) https://doi.org/10.1529/biophysj.106.084426

[6] Rosenmund, C., Stern-Bach, Y., Stevens, C.F.: The tetrameric structure of a glutamate receptor channel. Science **280**(5369), 1596–1599 (1998) https://doi.org/10.1126/science.280.5369.1596 https://www.science.org/doi/pdf/10.1126/science.280.5369.1596

[7] Carbone, A.L., Plested, A.J.R.: Superactivation of ampa receptors by auxiliary proteins. Nature Communications **7** (2016) https://doi.org/10.1038/ncomms10178 https://doi.org/10.1038/ncomms10178

[8] Pampaloni, N.P., Riva, I., Carbone, A.L., Plested, A.J.R.: Slow ampa receptors in hippocampal principal cells. Cell Reports **36** (2021) https://doi.org/10.1016/j.celrep.2021.109496 https://doi.org/10.1016/j.celrep.2021.109496

[9] Pampaloni, N.P., Plested, A.J.R.: Slow excitatory synaptic currents generated by ampa receptors. The Journal of Physiology **600**(2), 217–232 (2022) https://doi.org/10.1113/JP280877 https://physoc.onlinelibrary.wiley.com/doi/pdf/10.1113/JP280877

[10] Milstein, A.D., Zhou, W., Karimzadegan, S., Bredt, D.S., Nicoll, R.A.: Tarp subtypes differentially and dose-dependently control synaptic ampa receptor gating. Neuron **55**(6), 905–918 (2007) https://doi.org/10.1016/j.neuron.2007.08.022

[11] Milstein, A., Nicoll, R.: Regulation of ampa receptor gating and pharmacology by tarp auxiliary subunits. Trends in pharmacological sciences **29**, 333–9 (2008) https://doi.org/10.1016/j.tips.2008.04.004

[12] Cho, C.-H., St-Gelais, F., Zhang, W., Tomita, S., Howe, J.R.: Two families of tarp isoforms that have distinct effects on the kinetic properties of ampa receptors and synaptic currents. Neuron **55**(6), 890–904 (2007) https://doi.org/10.1016/j.neuron.2007.08.024

[13] Robert, A., Howe, J.R.: How ampa receptor desensitization depends

on receptor occupancy. Journal of Neuroscience **23**(3), 847–858 (2003) https://doi.org/10.1523/JNEUROSCI.23-03-00847.2003 https://www.jneurosci.org/content/23/3/847.full.pdf

[14] Devi, S.P.S., Cheng, Y., Tomita, S., Howe, J.R., Zhang, W.: Tarps modulate receptor-mediated paired-pulse depression and recovery from desensitization. Journal of Neuroscience **40**(43), 8233–8247 (2020) https://doi.org/10.1523/JNEUROSCI.3026-19.2020 https://www.jneurosci.org/content/40/43/8233.full.pdf

[15] Tsodyks, M., Pawelzik, K., Markram, H.: Neural networks with dynamic synapses. Neural Computation **10**(4), 821–835 (1998) https://doi.org/10.1162/089976698300017502 https://direct.mit.edu/neco/article-pdf/10/4/821/813807/089976698300017502.pdf

[16] Bowie, D., Lange, G.D.: Functional stoichiometry of glutamate receptor desensitization. The Journal of Neuroscience **22**, 3392–3403 (2002)

[17] Hodgkin, A.L., Huxley, A.F., Katz, B.: Measurement of current-voltage relations in the membrane of the giant axon of loligo. The Journal of Physiology **116**(4), 424–448 (1952) https://doi.org/10.1113/jphysiol.1952.sp004716 https://physoc.onlinelibrary.wiley.com/doi/pdf/10.1113/jphysiol.1952.sp004716

[18] Zhang, W., Devi, S.P.S., Tomita, S., Howe, J.R.: Auxiliary proteins promote modal gating of ampa- and kainate-type glutamate receptors. European Journal of Neuroscience **39**(7), 1138–1147 (2014) https://doi.org/10.1111/ejn.12519 https://onlinelibrary.wiley.com/doi/pdf/10.1111/ejn.12519

[19] Kato, A., Burris, K., Gardinier, K., Gernert, D., Porter, W., Reel, J., Ding, C., Tu, Y., Schober, D., Lee, M., Heinz, B., Fitch, T., Gleason, S., Catlow, J., Yu, H., Fitzjohn, S., Pasqui, F., Wang, H., Qian, Y., Witkin, J.: Forebrain-selective ampa-receptor antagonism guided by tarp γ-8 as an antiepileptic mechanism. Nature medicine **22** (2016) https://doi.org/10.1038/nm.4221

[20] Rogawski, M.A.: Ampa receptors as a molecular target in epilepsy therapy. Acta Neurologica Scandinavica **127**(s197), 9–18 (2013) https://doi.org/10.1111/ane.12099 https://onlinelibrary.wiley.com/doi/pdf/10.1111/ane.12099

[21] Witkin, J.M.: Targeted blockade of tarp-γ8-associated ampa receptors: Anticonvulsant activity with the selective antagonist ly3130481 (cerc-611). CNS & Neurological Disorders - Drug Targets **16**(10), 1099–1110 (2017) https://doi.org/10.2174/1871527316666171101132047